Geochemical Journal, Vol. 51, pp. 115 to 122, 2017 doi:10.2343/geochemj.2.0460

Hydrogen diffusion in the apatite-water system: Fluorapatite parallel to the *c*-axis

YOSHINORI HIGASHI,[1] SHOICHI ITOH,[1]* MINAKO HASHIGUCHI,[2] SHUHEI SAKATA,[1] TAKAFUMI HIRATA,[1] KEN WATANABE[3] and ISAO SAKAGUCHI[3]

[1]Division of Earth and Planetary Science, Kyoto University, Oiwakecho, Sakyo-ku, Kyoto-shi, Kyoto 606-8502, Japan
[2]Reserch Center for Planetary Organic Compounds, Kyushu University W1-A-622, 744, Motooka, Nishi-ku, Fukuoka 819-0395, Japan
[3]National Institute for Materials Science, 1-1 Namiki, Tsukuba, Ibaraki 305-0044, Japan

(*Received October 12, 2016; Accepted December 6, 2016*)

Many studies in the past decade have sought to explore the origin and evolution of water in planetary bodies based on the hydrogen isotopic compositions of apatite. However, no investigation has studied hydrogen diffusivity in apatite. This work reports hydrogen diffusion experiments using a natural Durango fluorapatite carried out under a saturated $^2H_2O/O_2$ vapor flow at temperatures of 500–700°C. Diffusion depth profiles for ^1H and ^2H were measured using secondary ion mass spectrometry (SIMS), indicating that ^2H diffusion occurred by an exchange reaction between the original ^1H and ^2H during annealing. Hydrogen diffusion coefficients were obtained by the fitting of diffusion profiles of ^2H using Fick's second law; they followed an Arrhenius-type relationship. The temperature dependence of hydrogen diffusion parallel to the *c*-axis at 500–700°C can be expressed as

$$D = 6.71 \times 10^{-13} \exp\left(-\frac{80.5 \pm 3.3}{RT}\right) \left[\mathrm{m}^2 / \mathrm{s}\right].$$

Hydrogen diffusion coefficients in apatite are several orders of magnitude greater than those of other elements. Hydrogen diffusion in apatite occurs at relatively low temperatures (below 700°C). This study indicates that the hydrogen isotopic compositions of apatite are readily affected by the presence of water vapor through the ^1H-^2H exchange reaction without changing the total water content in the crystal.

Keywords: apatite, hydrogen diffusion, H-D exchange, H_2O, SIMS

INTRODUCTION

Hydrous minerals are important because they provide information on the behavior of water during the formation and subsequent history of minerals and rocks (Suzuoki and Epstein, 1976). Their hydrogen isotopic compositions have been used as an important tracer of the isotopic composition of water (e.g., Taylor, 1977; Graham *et al*., 1984). However, without an understanding of hydrogen diffusivity in these hydrous minerals, it is difficult to estimate whether original hydrogen isotopic compositions from crystallization are preserved, or the subsequently modified by reactions with water after crystallization. Therefore, it is necessary to understand the hydrogen diffusivity in the mineral during water-rock interactions. For example, hydrogen diffusion has been investigated in hydrous minerals such as epidote, zoisite, muscovite (Graham, 1981), amphibole (Graham *et al*., 1984), ilvaite (Yaqian and Jibao, 1993), and tourmaline (Jibao and Yaqian, 1997).

Among the hydrous minerals, apatite-group minerals receive attention because they are able to survive in a wide range of geological settings on Earth and on extraterrestrial bodies such as the Moon, Mars, chondrites, and achondrites (McCubbin and Jones, 2015). Apatite, which is a calcium phosphate with the general formula $Ca_5(PO_4)_3(F,Cl,OH)$, has a hexagonal crystal structure, a = 9.4–9.6 Å, c = 6.8–6.9 Å, with a space group symmetry of $P6_3/m$ and sites bearing anions arranged along the *c*-axis (Hughes *et al*., 1989; Hughes and Rakovan, 2015). Apatite could contain various cations such as Ca, Pb, Sr, Ba and Mn in two of the cation site, and P, V and As in a third cation site (Hughes and Rakovan, 2015). The anion components of apatite, F, Cl and OH, can substitute for

*Corresponding author (e-mail: sitoh@kueps.kyoto-u.ac.jp)

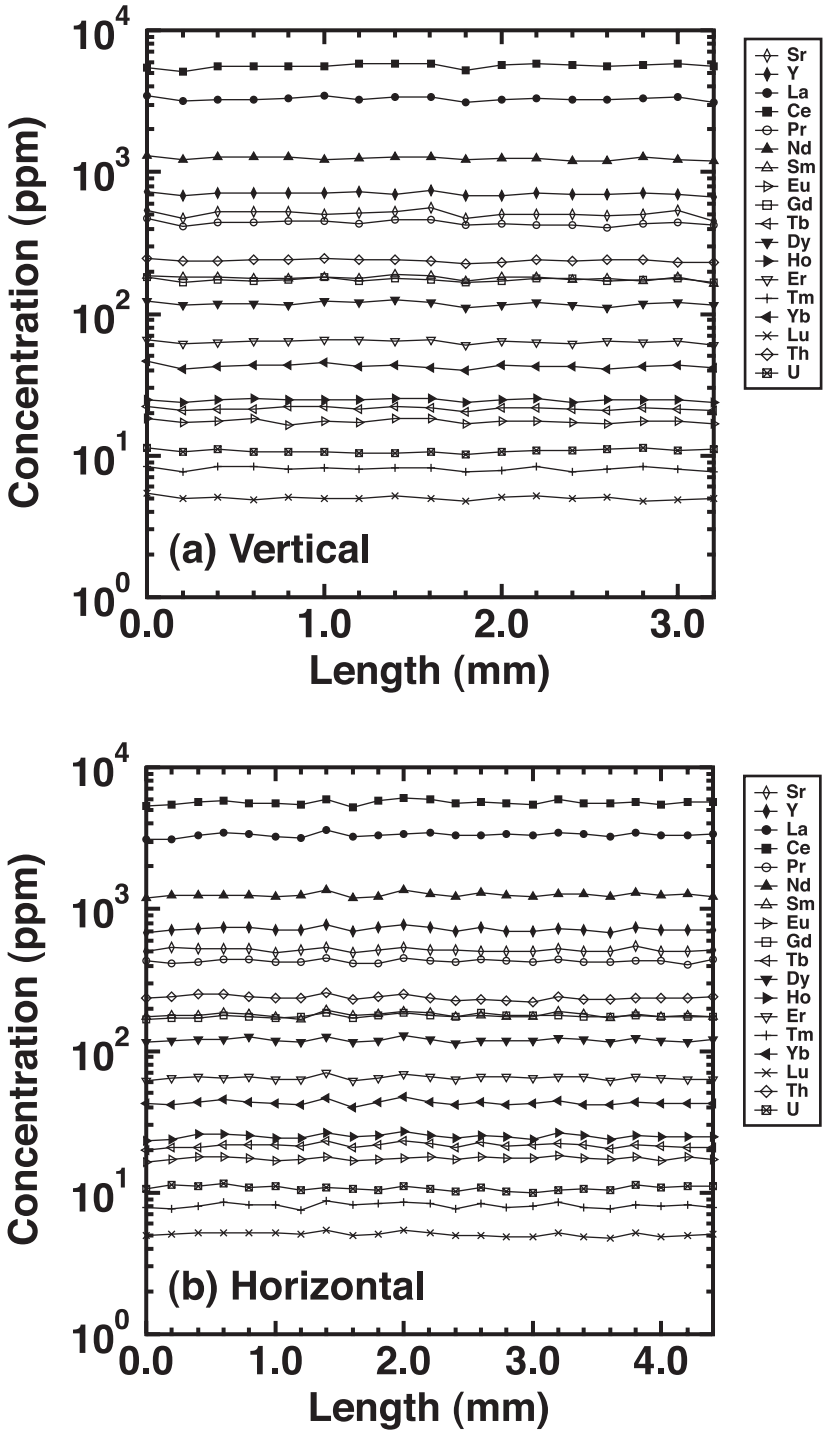

Fig. 1. Quantitative evaluation of trace elements in Durango apatite by LA-ICP-MS, (a) vertical 17 spots and (b) horizontal 23 spots. Trace elements are uniformly distributed in the c-plane of Durango apatite.

each other and apatite is called fluorapatite, chlorapatite and hydroxylapatite by the occupancy of the anion sites (Hughes *et al*., 1989). It contains highly volatile elements such as F, Cl, and OH in the anion sites, making it a useful recorder of volatile components and water in fluids and magmas (e.g., Boyce and Hervig, 2008, 2009; Marks *et al*., 2012; Harlov, 2015; McCubbin and Jones, 2015; Webster and Piccoli, 2015; Kusebauch *et al*., 2015). In the past decade, a number of publications have studied the origin and evolution of water in solar system bodies

by considering the hydrogen isotopic compositions of apatite (e.g., Greenwood *et al*., 2008, 2011; Barnes *et al*., 2013; Tartèse *et al*., 2013; Jones *et al*., 2014; Itoh *et al*., 2015; Usui *et al*., 2015; Singer *et al*., 2017).

However, no previous investigation has measured hydrogen diffusivity in apatite, in contrast to other hydrous minerals, despite such data being important in evaluating existing and future hydrogen isotopic analyses of apatite. Therefore, this study reports hydrogen diffusion experiments in apatite carried out under $^2H_2O/O_2$ vapor flows to estimate the hydrogen diffusivity of apatite and its temperature dependence. The use of $^2H_2O/O_2$ vapor is helpful in estimating the hydrogen diffusion as well as any variations in total hydrogen concentration in the apatite during water-rock interaction.

Experimental Procedure

Sample details and preparation

The sample selected for this study was a transparent natural hexagonal fluorapatite from Durango, Mexico. Durango apatite is easily obtained in large sizes and gem quality, and its mineralogy has been well studied (Young *et al*., 1969; Hughes *et al*., 1989; Sha and Chappell, 1999), making it the standard crystal used in studies of the physicochemical properties of apatite, including diffusion experiments (e.g., Farver and Giletti, 1989; Brenan, 1993; Cherniak, 2005). The chemical composition of the Durango fluorapatite, as reported by Young *et al*. (1969), is $Ca_{9.83}Na_{0.08}Sr_{0.01}RE_{0.09}(PO_4)_{5.87}(SO_4)_{0.05}(SiO_4)_{0.06}(AsO_4)_{0.01}(CO_3)_{0.01}F_{1.90}Cl_{0.12}(OH)_{0.01}$. The water content of Durango apatite is ~500 ppm H_2O (Greenwood *et al*., 2008).

Specimens of two Durango apatite crystals were cut normal to the *c*-axis into slabs about 1–2 mm thick using a low-speed diamond saw. Slices of samples were polished using several grades of diamond paste to obtain a mirror surface, and cleaned ultrasonically in deionized water and ethanol.

Impurity analyses by LA-ICP-MS

The variation of hydrogen diffusion coefficients in hydrous minerals could result from the differences in major elements of these minerals (Graham *et al*., 1984). Moreover, radioactive decay (e.g., nuclear fission) could affect diffusivity, as this would affect the defect concentration. Therefore, zoning of trace elements in apatite could influence the hydrogen diffusivity.

Since Boyce and Hodges (2005) report zoning of U and Th in Durango apatite, we evaluated the trace element abundances by traversal analysis using laser ablation inductively coupled plasma mass spectrometry (LA-ICP-MS) (Fig. 1). Trace element abundances were measured at Kyoto University, Japan, using a single-collector quadrupole ICP-MS (iCAP-Qc, Thermo Fischer Scientific, Bremen, Germany) coupled to an ArF excimer laser ablation system (NWR193, ESI, Portland, USA). We performed the analyses using a 50 μm spot size, a 5 Hz repetition rate, and 4.5 J/cm^2 fluence. The ICP-MS instrument was tuned to maximize the signal intensity of ^{139}La by changing the position of the plasma torch and the flow rate of the carrier gas (a mixture of He and Ar) while reducing the formation rate of $^{232}Th^{16}O^+$. After optimization of the ICP-MS, the apparent signal intensity of $^{232}Th^{16}O^+$ against $^{232}Th^+$ was *ca*. 0.6%. Two perpendicular traversal analyses were employed, and each traversal line consisted of 17 and 23 spot analyses with 200 μm step. The measurement at each spot consisted of (1) moving the stage to the target location; (2) surface cleaning with three laser pulses; (3) washing out the aerosol used in cleaning for 20 s; (4) acquiring a gas blank signal for 20 s; (5) ablating the sample for 30 s; and (6) waiting for 40 s while the baseline level stabilized. In total, 40 spots were analyzed. A silicate glass primary standard (NIST SRM610) for quantification (Pearce *et al*., 1997) was measured five times at the beginning of each sequence and also five times after 10 unknowns. Raw data were imported into Iolite 2.5 software (Paton *et al*., 2011; Woodhead *et al*., 2007, 2008). The software's data-reduction scheme reduced the raw data to obtain the concentrations of trace elements using the internal standard method and correct for instrumental drift. We used Ca (^{44}Ca) as an internal standard, assuming that CaO concentration in Durango apatite is 54.3 wt% (Douce *et al*., 2011). The overall uncertainties in the quantitative analysis were calculated based on error propagation of the external reproducibility of the E/^{44}Ca ratio (E: monitored isotopes such as ^{139}La) and the internal precision during single spot ablation. Uncertainties of the concentrations of trace element are quoted as twice the standard error, and were typically 4% to 5%. Among the rare earth elements, La, Ce, and Nd (~1000 ppm) were each present in concentrations of a few thousand ppm and were homogeneously distributed within the natural fluorapatite (mean square weighted deviation, MSWD values are 1.7, 1.8 and 2.5, respectively, n = 40). The trace elements appeared uniformly distributed in the *c*-plane of apatite, which is consistent with previous findings (Sha and Chappell, 1999).

Diffusion annealing experiment

Slices of apatite normal to the *c*-axis were used in the hydrogen diffusion experiments, which were carried out in a reactor at National Institute for Materials Science (NIMS, Tsukuba, Japan) that could independently control the temperature and humidity around the sample (Watanabe *et al*., 2013, 2014). Given that Durango apatite has an original H_2O content, heavy water (^2H_2O, >98%

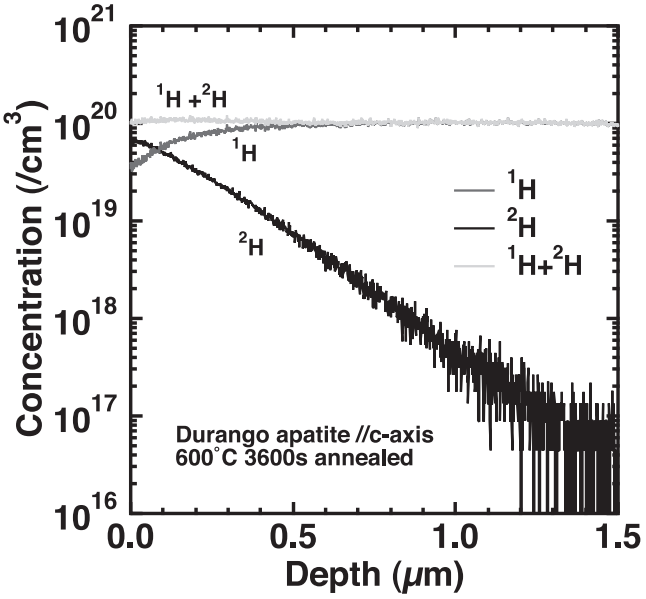

Fig. 2. Representative diffusion profile showing concentrations of ^{1}H, ^{2}H, and total hydrogen in Durango apatite annealed at 600°C for 3600 s.

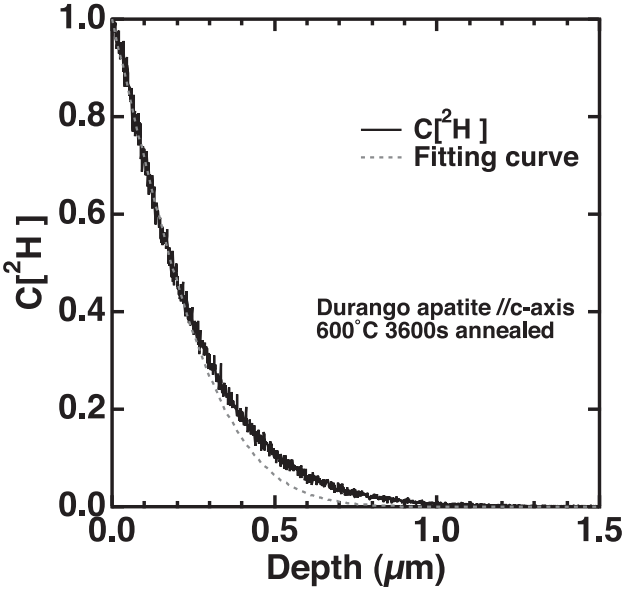

Fig. 3. Representative diffusion profile for ^{2}H concentration with depth in an apatite crystal from a hydrothermal run for 3600 s at 600°C, and the least squares linear regression fit to the data points.

^{2}H abundance) was employed as a diffusion source to determine hydrogen diffusivity. The apatite specimens were exposed to an oxygen carrier gas and the ^2H_2O gas (concentration 19.5%). A water reservoir was filled with ^2H_2O and maintained at 60°C. The flow rate of the oxygen carrier gas was ~600 sccm at 1 atm. Samples on a quartz glass boat, in a reactor initially completely filled with pure O_2 gas, underwent the isotope-exchange reaction in a humid gas mixture of O_2 and ^2H_2O. This experiment was designed to maintain a certain ^2H_2O gas concentration at the sample surface during annealing. The slices of apatite crystal were annealed at 500–700°C for 3600–5400 s using the heater; i.e., 5400 s at 500°C, 3600 s at 600°C, and 3600 s at 700°C.

SIMS analysis

After the diffusion experiments, hydrogen diffusion profiles were acquired by SIMS (Cameca ims 4f-E7 at LPS Kyoto University and Cameca ims 4f at NIMS). The diffusion profiles were obtained by depth profiling. To avoid charge accumulation on the surface, it was coated with Au (~20 nm) and irradiated by a rasterized $^{133}Cs^+$ primary ion beam with an acceleration voltage of +14.5 keV, intensity of ~5 nA, and spot size of about 10 μm. The primary beam was rasterized in a 100×100 μm area during irradiation. Secondary ions from the sputtering process were collected from the central area of 50×50 μm using a mechanical aperture to minimize artifacts. The intensities of the negative secondary ions $^1H^-$, $^2H^-$, and $^{18}O^-$ were measured. For charge compensation, a normal incident electron gun (with an accelerating voltage of 4.5 kV) was used to flood electrons onto the surface. To avoid contamination from residual hydrogen gas in the sample chamber, the vacuum was maintained below 8×10^{-8} Pa during measurements. The entrance and exit slits were narrowed enough to minimize the contribution of $^{16}O^2H^-$ to the $^{18}O^-$ reading. The depths of the SIMS craters were measured using a surface profiler (KLA_Tencor Alphastep D-120 and Kosaka Lab. Ltd. Surfcorder ET200) and laser microscope (KEYENCE VK-X-100). The secondary ion intensity profiles were converted to depth profiles.

Quantitative analysis of hydrogen in apatite

The concentration of hydrogen in the apatites for this diffusion experiment are estimated using ^{2}H ion implanted in the standard apatite sample. The relative sensitivity factor (RSF) (e.g., Homma *et al*., 1992) was obtained by analyzing the ^{2}H ions implanted in the sample slice (the same crystal as for the diffusion experiment) parallel to the *c*-axis using an ion implantation technique (Sakaguchi *et al*., 2003, 2004). The ^{2}H ions (37 keV acceleration voltage and 5×10^{14} ion/cm^2 implanted dose) were implanted at room temperature. The hydrogen concentration was calculated with the ratio of secondary ion intensities with $^1H/^{18}O$ and $^2H/^{18}O$. After the determination of RSF, the hydrogen concentration in two apatite crystals were estimated to be ~1×10^{20}/cm^3 and ~2.5×10^{20}/cm^3.

Table 1. Hydrogen diffusion coefficients in two apatite cystals

	T (°C)	Time (s)	D (m^2/s)	log$D$
Durango fluorapatite parallel to c				
Ap500_1α	500	5400	1.61×10^{-18}	−17.79
Ap500_2α	500	5400	2.65×10^{-18}	−17.58
Ap500_3α	500	5400	2.23×10^{-18}	−17.65
Ap500_4β	500	5400	3.28×10^{-18}	−17.48
Ap500_5β	500	5400	3.90×10^{-18}	−17.41
Ap500_6β	500	5400	2.01×10^{-18}	−17.70
Ap500_7β	500	5400	2.24×10^{-18}	−17.65
Average			$2.56 \pm 0.79 \times 10^{-18}$	-17.61 ± 0.13
Ap600_1α	600	3600	8.53×10^{-18}	−17.07
Ap600_2α	600	3600	6.62×10^{-18}	−17.18
Ap600_3α	600	3600	9.17×10^{-18}	−17.04
Ap600_4β	600	3600	1.26×10^{-17}	−16.90
Ap600_5β	600	3600	1.10×10^{-17}	−16.96
Average			$9.58 \pm 2.30 \times 10^{-18}$	-17.03 ± 0.11
Ap700_1α	700	3600	2.79×10^{-17}	−16.55
Ap700_2α	700	3600	2.96×10^{-17}	−16.53
Ap700_3α	700	3600	3.54×10^{-17}	−16.45
Ap700_4β	700	3600	3.77×10^{-17}	−16.42
Average			$3.27 \pm 0.47 \times 10^{-17}$	-16.49 ± 0.06

α and β: These symbols designate the different crystal. Total hydrogen concentration of α is ~2.5×10^{20} (/cm^3) and that of β is ~1×10^{20} (/cm^3).

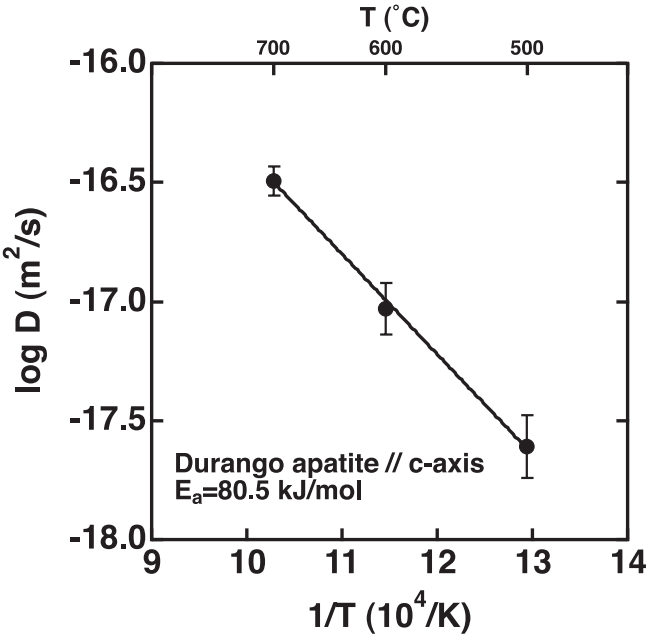

Fig. 4. Arrhenius plot of hydrogen self-diffusion in apatite, showing the results for diffusion experiments in natural Durango apatite measured for diffusion parallel to the c-axis. The line is a least-squares fit to the diffusion data. The fit of Eq. (2) to the experimental data for hydrogen diffusivity in apatite at 1 atm yields an activation energy of 80.5 ± 3.3 kJ mol^{-1} and a pre-exponential factor of 6.71 × 10^{-13} m^2 s^{-1}. Each symbol is the average value of each temperature (Table 1). The errors are 1σ.

Diffusion analysis

To determine the diffusion coefficient (D), the C[^{2}H] profile was fitted using the solution of the diffusion equation obtained by assuming a constant concentration of ^{2}H at the sample surface and diffusion in a semi-infinite medium (Crank, 1975). The diffusion profiles were fitted to Eq. (1) using least squares:

$$\left(\frac{C_{(x,t)} - C_0}{C_s - C_0}\right) = erfc\left(\frac{x}{2\sqrt{Dt}}\right) \quad (1)$$

where $C_{(x,t)}$ is the concentration at distance x from the surface, C_s is the surface concentration, C_0 is the background concentration, and x is the penetration depth. D is the diffusion coefficient, t is the duration of the diffusion treatment, and $erfc = 1 - erf$ (where erf is the Gaussian error function).

RESULTS

Diffusion profiles of ^{1}H and ^{2}H in apatite

Figure 2 shows a representative diffusion profile for the concentrations of ^{1}H and ^{2}H, and also total hydrogen concentration, in Durango apatite annealed at 600°C for 3600 s. The concentrations of ^{1}H and ^{2}H starting at the surface are 3×10^{19} and 7×10^{19}/cm^3, respectively. The ^{1}H concentration increased with increasing depth, eventually reaching the original hydrogen concentration of 1×10^{20}/cm^3. The ^{2}H concentration decreased with increasing depth. The constant total hydrogen concentration ($1 \pm 0.04 \times 10^{20}$/cm^3 ($2\sigma$)) throughout the sample shows that ^{2}H diffusion occurred via its initial exchange with the original surface hydrogen and subsequent diffusion in the lattice by a simple ^{1}H-^{2}H exchange mechanism. Similar profiles were obtained at the other considered temperatures (500 and 700°C). Therefore, to estimate the hydrogen diffusion coefficient in the apatite lattice at each temperature, the intensity ratio $^2H^-/(^1H^- + ^2H^-)$ (denoted as C[^{2}H]) in the profile was fitted for use in the calculation of the diffusion equation (1) (Fig. 3). The fitted values show a good agreement in the surface region of up to about 200 nm depth. The obtained hydrogen diffusion coefficients at the different temperatures are listed in Table 1.

Temperature dependence of hydrogen diffusion in apatite

Diffusion coefficients (D) generally follow the Arrhenius equation:

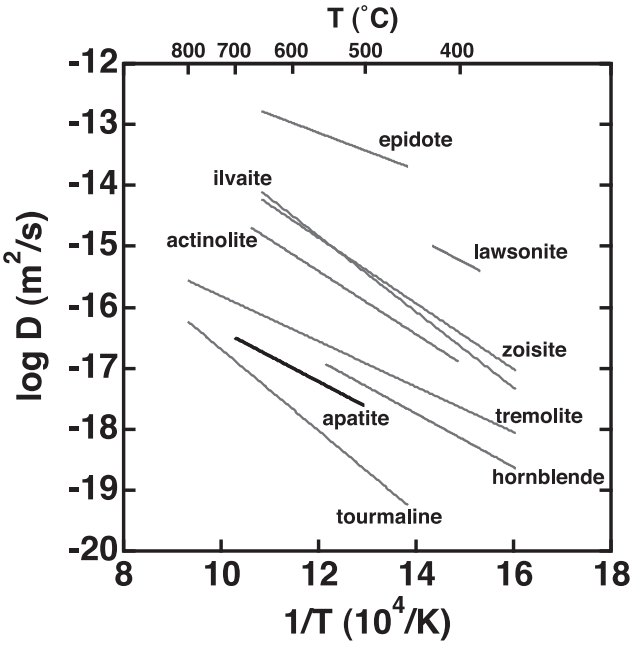

Fig. 5. Comparison of hydrogen diffusion for apatite (black line) and hydrous minerals (gray lines; Ingrin and Blanchard, 2006). Sources for data: epidote (Graham, 1981); lawsonite (Marion et al., 2001); zoisite (Graham, 1981); ilvaite (Yaqian and Jibao, 1993); actinolite (Graham et al., 1984 from Suzuoki and Epstein, 1976); tremolite (Graham et al., 1984); hornblende (Graham et al., 1984); tourmaline (Jibao and Yaqian, 1997); apatite (this study).

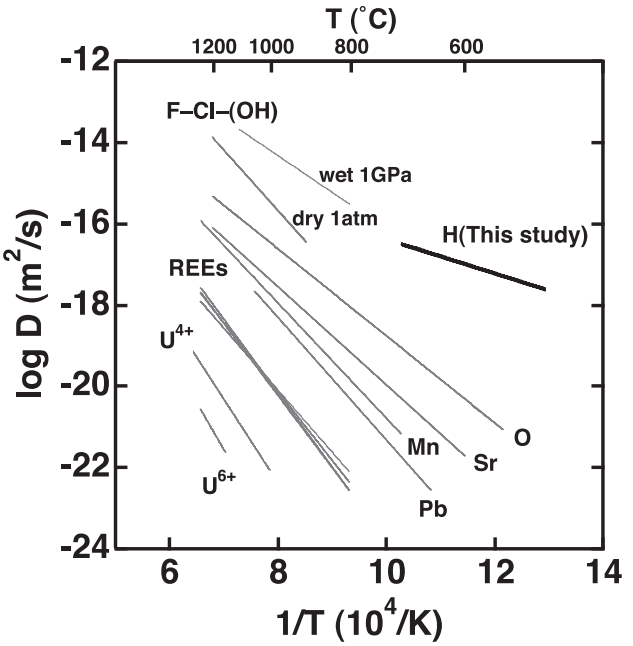

Fig. 6. Summary of diffusion data for cations and anions in apatite. Gray lines are previously reported values, and the black line indicates data of the present study. Sources for data: F-Cl-(OH) (Brenan, 1993); O (Farver and Giletti, 1989); Sr (Cherniak and Ryerson, 1993); Pb (Cherniak et al., 1991); REEs (Cherniak, 2000); U and Mn (Cherniak, 2005); H (this study).

$$D = D_0 \exp\left(-\frac{E_a}{RT}\right) \qquad (2)$$

where D_0 is the pre-exponential factor, E_a is the activation energy for diffusion, and T is the temperature. In the present study, the Arrhenius relation for the hydrogen diffusion in apatite was calculated using the average value of diffusion coefficients from two apatite crystals at each temperature (Table 1). Figure 4 shows that an Arrhenius relation was obtained for hydrogen diffusion in Durango apatite parallel to the *c*-axis at 500–700°C:

$$D = 6.71 \times 10^{-13} \exp\left(-\frac{80.5 \pm 3.3}{RT}\right) \left[\mathrm{m}^2 / \mathrm{s}\right]. \qquad (3)$$

Discussion

Hydrogen diffusivity in apatite and hydrous minerals

Hydrogen diffusion in hydrous minerals is important because it can help us to understand the formation and hydrothermal history of minerals and rocks. Several previous studies have reported hydrogen diffusion in hydrous minerals, and their findings were reviewed by Ingrin and Blanchard (2006). The hydrogen diffusivities obtained in the present study for apatite and those for various other hydrous minerals under hydrothermal conditions from Ingrin and Blanchard (2006) are shown in Fig. 5. The other diffusivity data were also obtained from ^{1}H-^{2}H exchange experiments. The diffusivities vary considerably, by about five orders of magnitude. Hydrogen diffusivity in apatite is relatively slow compared with the other hydrous minerals. Diffusivity generally depends on the number of effective sites, and the variation in Fig. 5 could be explained by the OH contents of the various hydrous minerals. This suggests that the OH content of apatite could increase hydrogen diffusion rates.

The activation energies for hydrogen diffusion in these minerals show less variation, and are in the range of 80 to 120 kJ/mol (Ingrin and Blanchard, 2006). The similar activation energies suggest that hydrogen diffusion occurs by the same mechanism in each case. Hydrogen incorporated into the lattice migrates mainly as a single proton much as in oxides and silicates, jumping between successive OH positions (Norby and Larring, 1997; Ingrin and Blanchard, 2006). Considering that OH is stable in hydrous minerals, the incorporated hydrogen diffuses by displacing H originally bonded with O via the Grotthus mechanism (Marion *et al.*, 2001). The activation energy for hydrogen diffusion comprises two contributions: the

energy needed to break the original O-H bond and the migration energy of hydrogen diffusion between OH sites in the lattice. Therefore, the crystal structure has been suggested to make only a small contribution to the activation energy of hydrogen diffusion in hydrous minerals. Moreover, this suggests that variation in OH content of apatite will not lead to large changes in the activation energy for hydrogen diffusion.

Comparison with the diffusivities of other elements in apatite

For hydrogen diffusion data in apatite to be important to geochemical and cosmochemical research, it has to be analyzed in comparison with the diffusion coefficients of other major components of the halogen site such as F and Cl, as well as OH. The diffusion coefficients of various cations and anions in apatite have been reported previously (e.g., Farver and Giletti, 1989; Brenan, 1993; Cherniak, 2005), and are plotted in Fig. 6. The diffusion rate of hydrogen in apatite in this study is several orders of magnitude higher than that of the other elements, and the activation energy for hydrogen diffusion is lower than that for the other anions and cations, especially F and Cl. If OH diffusion in apatite is similar to F and Cl diffusion (Brenan, 1993), hydrogen diffusion in apatite is more than three orders of magnitude faster than hydroxyl diffusion at 500–700°C. This is also consistent with our result that the hydrogen isotopic compositions of apatite could be easily affected by water through the ^{1}H-^{2}H exchange reaction without changing the total water content (Fig. 2). The hydrogen isotopic composition of apatite is therefore a sensitive indicator of water-mineral interactions in the Earth and extraterrestrial bodies.

Summary

SIMS was used to measure depth profiles of ^{1}H and ^{2}H concentrations after hydrothermal hydrogen diffusion experiments in natural Durango fluorapatite. The diffusion coefficients along the crystallographic *c*-axis in apatite at 500–700°C were found to follow the expression

$$D = 6.71 \times 10^{-13} \exp\left(-\frac{80.5 \pm 3.3}{RT}\right) \left[\mathrm{m}^2 / \mathrm{s}\right].$$

The diffusion profiles revealed the extent of the exchange of the original ^{1}H by ^{2}H during annealing. The diffusion coefficients of hydrogen in apatite are several orders of magnitude higher than those reported for other elements; the activation energy of hydrogen diffusion is lower than those of other elements. As a result, this study indicates that the hydrogen isotopic compositions of apatite could be altered from the original isotopic compositions through the ^{1}H-^{2}H exchange reaction between water vapor and mineral without changing the water content after crystallization.

Acknowledgments—The authors appreciate the associate editor of Dr. J. P. Greenwood and anonymous reviewer for constructive reviews of this manuscript. This work was partly supported by Grants-in-Aid for Scientific Research (No. JP25108006, JP26247094, JP16H02267 and JP16H01118) to S.I. from the Japan Society for the Promotion of Science.

References

Barnes, J. J., Franchi, I. A., Anand, M., Tartèse, R., Starkey, N. A., Koike, M., Sano, Y. and Russell, S. S. (2013) Accurate and precise measurements of the D/H ratio and hydroxyl content in lunar apatites using NanoSIMS. *Chem. Geol.* **337–338**, 48–55.

Boyce, J. W. and Hodges, K. V. (2005) U and Th zoning in Cerro de Mercado (Durango, Mexico) fluorapatite: Insight regarding the impact of recoil redistribution of radioactive ^{4}He on (U-Th)/He thermochronology. *Chem. Geol.* **219**, 261–274.

Boyce, J. W. and Hervig, R. L. (2008) Magmatic degassing histories from apatite volatile stratigraphy. *Geology* **36**, 63–66.

Boyce, J. W. and Hervig, R. L. (2009) Apatite as a monitor of late-stage magmatic processes as Volcán Irazú, Costa Rica. *Contrib. Mineral. Petrol.* **157**, 135–145.

Brenan, J. (1993) Kinetics of fluorine, chlorine and hydroxyl exchange in fluorapatite. *Chem. Geol.* **110**, 195–210.

Cherniak, D. J. (2000) Rare earth element diffusion in apatite. *Geochim. Cosmochim. Acta* **64**, 3871–3885.

Cherniak, D. J. (2005) Uranium and manganese diffusion in apatite. *Chem. Geol.* **219**, 297–308.

Cherniak, D. J. and Ryerson, F. J. (1993) A study of strontium diffusion in apatite using Rutherford backscattering spectroscopy and ion implantation. *Geochim. Cosmochim. Acta* **57**, 4653–4662.

Cherniak, D. J., Lanford, W. A. and Ryerson, F. J. (1991) Lead diffusion in apatite and zircon using ion implantation and Rutherford Backscattering techniques. *Geochim. Cosmochim. Acta* **55**, 1663–1673.

Crank, J. (1975) *The Mathematics of Diffusion*. Clarendon, Oxford, 414 pp.

Douce, A. E. P., Roden, M. F., Chaumba, J., Fleisher, C. and Yogodzinski, G. (2011) Compositional variability of terrestrial mantle apatites, thermodynamic modeling of apatite volatile contents, and the halogen and water budgets of planetary mantles. *Chem. Geol.* **288**, 14–31.

Farver, J. R. and Giletti, B. J. (1989) Oxygen and strontium diffusion kinetics in apatite and potential applications to thermal history determinations. *Geochim. Cosmochim. Acta* **53**, 1621–1631.

Graham, C. M. (1981) Experimental hydrogen isotope studies III: Diffusion of hydrogen in hydrous minerals, and stable isotope exchange in metamorphic rocks. *Contrib. Mineral. Petrol.* **76**, 216–228.

Graham, C. M., Harmon, R. S. and Sheppard, S. M. F. (1984) Experimental hydrogen isotope exchange between

amphibole and water. *Amer. Mineral*. **69**, 128–138.

Greenwood, J. P., Itoh, S., Sakamoto, N., Vicenzi, E. P. and Yurimoto, H. (2008) Hydrogen isotope evidence for loss of water from Mars through time. *Geophys. Res. Lett*. **35**, 1–5.

Greenwood, J. P., Itoh, S., Sakamoto, N., Warren, P., Taylor, L. and Yurimoto, H. (2011) Hydrogen isotope ratios in lunar rocks indicate delivery of cometary water to the Moon. *Nat. Geosci*. **4**, 79–82.

Harlov, D. E. (2015) Apatite: a fingerprint for metasomatic processes. *Elements* **11**, 171–176.

Homma, Y., Yamawaki, M., Igo, A. and Ochiai, S. (1992) Stability of relative sensitivity factors in secondary ion mass spectrometry. *J. Mass Spectr. Jpn*. **40**, 217–223.

Hughes, J. M. and Rakovan, J. F. (2015) Structurally robust, chemically diverse: apatite and apatite supergroup minerals. *Elements* **11**, 165–170.

Hughes, J. M., Cameron, M. and Crowley, K. D. (1989) Structural variations in natural F, OH, and Cl apatites. *Amer. Mineral*. **74**, 870–876.

Ingrin, J. and Blanchard, M. (2006) Diffusion of hydrogen in minerals. *Rev. Mineral. Geochem*. **62**, 291–320.

Itoh, S., Hashiguchi, M., Sakaguchi, I., Sakata, S. and Hirata, T. (2015) Hydrogen diffusion experiment of apatite crystal. *Goldschmidt Conference Abstract*, p. 1394.

Jibao, G. and Yaqian, Q. (1997) Hydrogen isotope fractionation and hydrogen diffusion in the tourmaline-water system. *Geochim. Cosmochim. Acta* **61**, 4679–4688.

Jones, R. H., McCubbin, F. M., Dreeland, L., Guan, Y., Burger, P. V. and Shearer, C. K. (2014) Phosphate minerals in LL chondrites: A record of the origin of fluids during metamorphism on ordinary chondrite parent bodies. *Geochim. Cosmochim. Acta* **132**, 120–140.

Kusebauch, C., John, T., Whitehouse, M. J. and Engvik, A. K. (2015) Apatite as probe for the halogen composition of metamorphic fluids (Bamble Sector, SE Norway). *Contrib. Mineral. Petrol*. **170**, 34.

Marion, S., Meyer, H. W., Carpenter, M. and Norby, T. (2001) H_2O-D_2O exchange in lawsonite. *Amer. Mineral*. **86**, 1166–1169.

Marks, M. A. W., Wenzel, T., Whitehouse, M. J., Loose, M., Zack, T., Barth, M., Worgard, L., Krasz, V., Eby, G. N., Stosnach, H. and Markl, G. (2012) The volatile inventory (F, Cl, Br, S, C) of magmatic apatite: An integrated analytical approach. *Chem. Geol*. **291**, 241–255.

McCubbin, F. M. and Jones, R. H. (2015) Extraterrestrial apatite: Planetary geochemistry to astrobiology. *Elements* **11**, 183–188.

Norby, T. and Larring, Y. (1997) Concentration and transport of protons in oxides. *Curr. Opin. Solid State Mat. Sci*. **2**, 593–599.

Paton, C., Hellstrom, J., Paul, B., Woodhead, J. and Hergt, J. (2011) Iolite: Freeware for the visualisation and processing of mass spectrometric data. *J. Anal. Atom. Spectrom*. **26**, 2508–2518.

Pearce, N. J. G., Perkins, W. T., Westgate, J. A., Gorton, M. P., Jackson, S. E., Neal, C. R. and Chenery, S. P. (1997) A compilation of new and published major and trace element data for NIST SRM 610 and NIST SRM 612 glass reference materials. *Geostand. Newsl*. **21**, 115–144.

Sakaguchi, I., Park, D., Takata, Y., Hishita, S., Ohashi, N., Haneda, H. and Mitsuhashi, T. (2003) An effect of annealing on In implanted ZnO. *Nucl. Instrum. Methods Phys. Res. Section B* **206**, 153–156.

Sakaguchi, I., Sato, Y., Park, D., Ohashi, N., Haneda, H. and Hishita, S. (2004) Recovery of the luminescence property in sulfur-implanted ZnO thin film. *Nucl. Instrum. Methods Phys. Res. Section B* **217**, 417–422.

Sha, L.-K. and Chappell, B. (1999) Apatite chemical composition, determined by electron microprobe and laser-ablation inductively coupled plasma mass spectrometry, as a probe into granite petrogenesis. *Geochim. Cosmochim. Acta* **63**, 3861–3881.

Singer, J. A., Greenwood, J. P., Itoh, S., Sakamoto, N. and Yurimoto, H. (2017) Evidence for the solar wind in lunar magmas: A study of slowly cooled samples of the Apollo 12 olivine basalt suite. *Geochem. J*. **51**, this issue, 95–104.

Suzuoki, T. and Epstein, S. (1976) Hydrogen isotope fractionation between OH-bearing minerals and water. *Geochim. Cosmochim. Acta* **40**, 1229–1240.

Tartèse, R., Anand, M., Barnes, J. J., Starkey, N. A., Franchi, I. A. and Sano, Y. (2013) The abundance, distribution, and isotopic composition of Hydrogen in the Moon as revealed by basaltic lunar samples: Implications for the volatile inventory of the Moon. *Geochim. Cosmochim. Acta* **122**, 58–74.

Taylor, H. P. (1977) Water/rock interactions and the origin of H_2O in granitic batholiths. *J. Geol. Soc*. **133**, 509–558.

Usui, T., Alexander, C. M. O. D., Wang, J., Simon, J. I. and Jones, J. H. (2015) Meteoritic evidence for a previously unrecognized hydrogen reservoir on Mars. *Earth Planet. Sci. Lett*. **410**, 140–151.

Watanabe, K., Lee, D. H., Sakaguchi, I., Nomura, K., Kamiya, T., Haneda, H., Hosono, H. and Ohashi, N. (2013) Surface reactivity and oxygen migration in amorphous indium-gallium-zinc oxide films annealed in humid atmosphere. *Appl. Phys. Lett*. **103**, 201904.

Watanabe, K., Hashiguchi, M., Sakaguchi, I., Bryant, A., Adachi, Y., Zhen, Y., Ohgaki, T., Ohsawa, T., Haneda, H. and Ohashi, N. (2014) Hydrogen in tin dioxide films and bulk ceramics: An attempt to identify the most hidden impurity. *Appl. Phys. Lett*. **104**, 042110.

Webster, J. D. and Piccoli, P. M. (2015) Magmatic apatite: A powerful, yet deceptive, mineral. *Elements* **11**, 177–182.

Woodhead, J., Hellstrom, J., Hergt, J., Greig, A. and Maas, R. (2007) Isotopic and elemental imaging of geological materials by laser ablation inductively coupled plasma-mass spectrometry. *J. Geostand. Geoanal. Res*. **31**, 331–343.

Woodhead, J., Hellstrom, J., Paton, C., Hergt, J., Greig, A. and Maas, R. (2008) A guide to depth profiling and imaging applications of LA-ICP-MS. *Laser Ablation ICP-MS in the Earth Sciences: Current Practices and Outstanding Issues* (Sylvester, P., ed.), *Mineralogical Association of Canada Short Course Series* **40**, 135–145.

Yaqian, Q. and Jibao, G. (1993) Study of hydrogen isotope equilibrium and kinetic fractionation in the ilvaite-water system. *Geochim. Cosmochim. Acta* **57**, 3073–3082.

Young, E. J., Myers, A. T., Munson, E. L. and Conklin, N. M. (1969) Mineralogy and geochemistry of fluorapatite from Cerro de Mercado, Durango, Mexico. *U.S. Geological Survey Professional Paper* **650-D**, D84–D93.